



Contents lists available at ScienceDirect



Catalysis Today

journal homepage: www.elsevier.com/locate/cattod

Enhancement of methanation of carbon dioxide using dielectric barrier discharge on a ruthenium catalyst at atmospheric conditions

Chung Jun Lee^a, Dae Hoon Lee^b, Taegyu Kim^{a,*}

^a Department of Aerospace Engineering, College of Engineering, Chosun University 309 Pilmun-daero, Dong-gu, Gwangju 61452, Republic of Korea

^b Industrial Plasma Laboratory, Korea Institute of Machinery and Materials, 156 Gajeonbuk-ro, Yuseong-gu, Daejeon 34103, Republic of Korea

ARTICLE INFO

Article history:

Received 23 August 2016

Received in revised form 2 January 2017

Accepted 14 January 2017

Available online xxx

Keywords:

Carbon dioxide

Methanation

Power to gas

Dielectric barrier discharge plasma

Ruthenium

Optical emission spectroscopy

ABSTRACT

This paper describes the enhancement of CO₂ methanation using dielectric barrier discharge (DBD) on Ru catalyst under atmospheric conditions. The DBD plasma leads to increased deoxygenation of CO₂, which is decomposed into CO. Subsequently, the Ru catalyst activates the methanation in the DBD plasma at atmospheric conditions. The effect of the discharge frequency of the DBD plasma and the H₂/CO₂ mixture ratio on the CO₂ conversion and CH₄ selectivity is investigated. The CO₂ conversion and CH₄ selectivity rapidly increase at a discharge frequency above 2.5 kHz, and reach 23.20% and 95.02%, respectively, when the H₂/CO₂ molar ratio is 7. CO₂ methanation and deoxygenation are simultaneously enhanced by adding Ar. Optical emission spectroscopy is used for the plasma diagnostics in the CO₂ methanation process. The optical emission spectra of the γ-Al₂O₃ and Ru/γ-Al₂O₃ catalysts are measured to investigate the effect of the presence of Ru during plasma generation. Finally, the excited and ionized hydrogen atoms are confirmed as the primary accelerators in the plasma-assisted CO₂ methanation process.

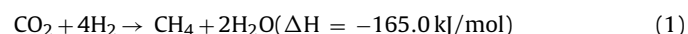
© 2017 Elsevier B.V. All rights reserved.

1. Introduction

Recently, methanation of CO₂ has become an important challenge. CO₂ methanation is important for two reasons: the first is CO₂-related environmental issues and the second is the potential of the “power to gas (P2G)” process [1,2]. Since the industrial revolution, atmospheric concentration of CO₂ has continuously increased; the increased CO₂ concentration causes climate change and global warming [3,4]. The major source of CO₂ emissions is from the combustion of fossil fuels, such as in an internal combustion engine. However, human beings cannot stop using fossil fuels to prevent CO₂ emissions because the modern human lifestyle is highly dependent on the fossil fuel-based economy. For this reason, reasonable and alternative solutions to reduce CO₂ emissions involve recycling or utilizing the emitted CO₂.

Either recycling or utilizing CO₂ can be achieved by the Sabatier reaction. The Sabatier reaction is a well-known process to convert

CO₂ into useful products, such as CH₄ and H₂O, according to the process shown in Eq. (1),



The CO₂ methanation process has a great potential for environmental, industrial, and economical applications because fuels or fuel sources can be regenerated from the waste CO₂ gas. Based on the renewable energy growth, CO₂ methanation can be used for the P2G process that converts electrical power to a gas fuel. It means that the excess power can be utilized and stored in a storable gas state, such as CH₄.

For this reason, the CO₂ methanation process has been widely studied. Typically, CO₂ methanation has been achieved for group VIII-based metal catalysts, such as Ni and Ru [5–9]. However, the catalytic methanation process using the Sabatier reaction is usually activated above 300 °C and 20 bar [10–12]. The temperature and pressure requirements make the process complex because a heater, pressurization device, and pressurized reactor are required. It means that the system has a limitation for miniaturization and simplification, which limits its applicability to various industrial applications. Therefore, an alternative approach to lower the temperature and pressure to activate the CO₂ methanation process is required.

Recently, non-thermal plasma-assisted processes have been proposed for various reactions, including treatment, decomposition, conversion, and reforming processes. Many studies have

Abbreviations: DBD, dielectric barrier discharge; OES, optical emission spectroscopy; P2G, power to gas; SED, specific energy density.

* Corresponding author.

E-mail address: taegyu@chosun.ac.kr (T. Kim).

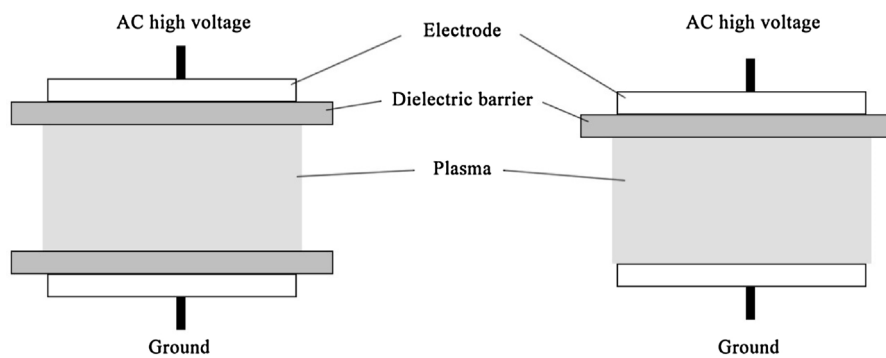


Fig. 1. Typical configuration for dielectric barrier discharge.

reported that the non-thermal plasma-assisted process provides a synergistic effect between the plasma and catalyst. The surfaces of the catalysts were pretreated by the non-thermal plasma to enhance their catalytic performance; this surface-modifying treatment also improved the durability of the catalysts [13–17]. The enhancement of the catalytic performance using the non-thermal plasma was also reported for pollutant removal and reforming species, such as methanol and methane [18–28].

The non-thermal plasma has many advantages in various chemical processes. A few groups have reported the study of CO and CO₂ hydrogenation using a non-thermal plasma [29–32]. Therefore, the non-thermal plasma-assisted CO₂ methanation process was investigated in this study. Among the non-thermal plasma techniques, dielectric barrier discharge (DBD) was used to generate the plasma on the catalyst. The activation and enhancement of the CO₂ methanation in the plasma at atmospheric conditions were verified, and the mechanism between the plasma and catalyst was investigated in this study.

2. Experiments

2.1. Catalyst preparation

Ru is a popular catalyst in the chemical industry. For example, Ru-promoted cobalt catalysts have been commonly used for energy conversion processes, such as Fischer-Tropsch synthesis and the CO₂ methanation process [33–35]. Therefore, Ru was selected as the catalyst for the DBD plasma-assisted CO₂ methanation process in this study. The Ru chloride powder (RuCl₃·3H₂O, >99% purity) and alumina spheres (γ -Al₂O₃, 1/16 inches) that are used as the catalyst support were purchased from Kojima Chemicals and Strem Chemicals, respectively. The Ru powder was dissolved in distilled water, and the solution was added to the γ -Al₂O₃ support. The impregnated catalyst was dried at room temperature for 24 h. After drying, the catalyst was calcined at 350 °C for 2 h; as a result, the Ru/ γ -Al₂O₃ catalyst was obtained.

In plasma catalysis, the catalyst is exposed to the plasma streamer. Thus, the catalyst can influence the generation and propagation of the plasma streamer. When the streamer is generated, it would first be in contact with the surface layer of the catalyst. Without sufficient catalyst loading, the probability for interaction between the streamer and the catalyst would be reduced. The loading fraction of Ru in the Ru/ γ -Al₂O₃ catalyst was 5.369 wt%, which is enough for the streamer to be in contact with the catalyst when propagated.

2.2. DBD plasma-catalytic reactor

DBD is a method for plasma generation that requires a dielectric barrier material between the electrodes, as shown in Fig. 1 [36].

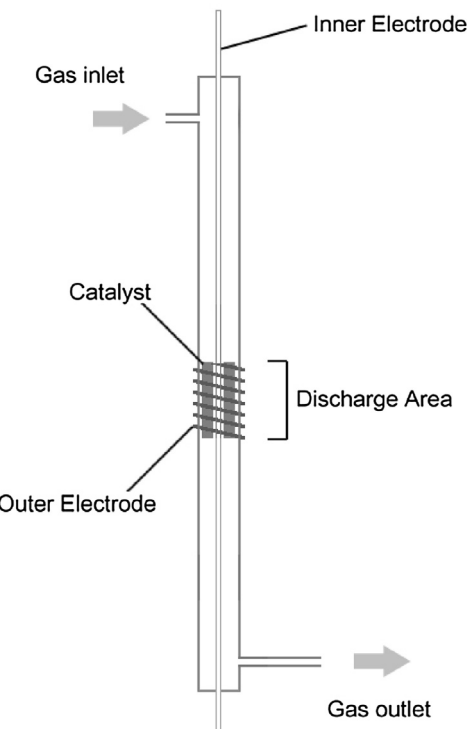


Fig. 2. Schematic of the dielectric barrier discharge plasma reactor.

The quartz glass tube was used as the dielectric barrier because it is not reactive with other substances and its high dielectric constant can sustain the discharge. The configuration of the DBD plasma-catalytic reactor is shown in Fig. 2. The reactor consists of a quartz glass tube and two electrodes. The quartz glass has an axis-symmetrical shape with dimensions of 402 mm (length), 13 mm (outer diameter), and 10.9 mm (inner diameter). The stainless steel fittings were connected on both ends of the reactor, which was used for the gas supply.

The reactor has two electrodes: one is a stainless steel rod and the other is a helical steel wire. The stainless steel rod was installed inside the reactor to align with the center axis of the reactor, and the steel wire was installed around the outside of the reactor. The steel wire electrode was 45 mm long in the axial direction of the quartz tube. The plasma was generated in the space between the two electrodes. Thus, the prepared catalysts were filled in this space, which was matched with the plasma discharge volume. The plasma was generated in the same volume in which the catalysts of 3 g were packed. Glass wool was used to fix the catalysts in the predetermined location. The reactor was installed vertically with respect to the ground to remove water gravitationally from the plasma dis-

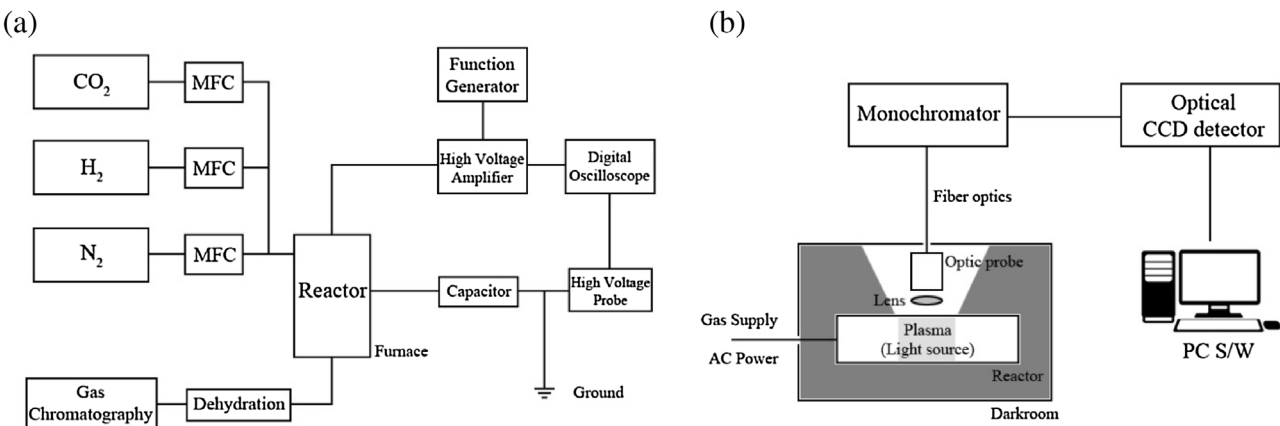


Fig. 3. Schematic diagrams of the experimental apparatus for (a) the methanation experiment and (b) optical emission spectroscopy experiment.

Table 1

Effect of the presence of the Ru/ γ -Al₂O₃ catalyst on CO₂ methanation under the dielectric barrier discharge (DBD) plasma at 3 kHz and 9 kV.

	CO ₂ Conversion (%)		CH ₄ Selectivity (%)		CO Selectivity (%)	
	No Catalyst	Ru/ γ -Al ₂ O ₃	No Catalyst	Ru/ γ -Al ₂ O ₃	No Catalyst	Ru/ γ -Al ₂ O ₃
DBD Off	0.03	0.01	0.15	0.10	0.13	0.01
DBD On	8.21	12.80	1.42	73.30	43.84	5.12

charge area and catalyst bed, and a gas downflow configuration was used.

2.3. Experimental apparatus

The schematic diagrams of the experimental apparatus are shown in Fig. 3, including the plasma reactor setup to perform the CO₂ methanation under plasma generation (Fig. 3(a)), and the optical emission spectroscopy (OES) setup to analyze the plasma characteristics during the plasma-catalytic reaction (Fig. 3(b)). An identical reactor was used for CO₂ methanation and OES analysis of the plasma generation.

A high voltage was applied to the reactor to generate the DBD plasma on the catalyst. The voltage waveform was applied using a function generator (Agilent 33220A), and the applied voltage was amplified using a high-voltage amplifier (Trek Model 20/20C). The electrical discharge characteristics, such as the onset voltage and frequency of the discharge, were measured by a high-voltage probe (Tektronix P6015A) and digital oscilloscope (LeCroy WaveSurfer 424). The capacitor (1024 pF) was connected to the gap capacitance between the electrodes in series to analyze the discharge power. The discharge power was calculated using the V-Q Lissajous method. Fig. 4 shows a V-Q Lissajous diagram of the DBD plasma discharged on Ru/ γ -Al₂O₃ at 9 kV and 3 kHz. The preliminary tests confirmed that the onset voltage of the discharge was 9 kV and that the arc transition occurred as the discharge frequency increased above 2 kHz at a discharge voltage above 9 kV. The change of the discharge frequency was a more dominant factor to determine the performance than the discharge voltage. Therefore, the discharge voltage was fixed at 9 kV for all experiments.

A mass flow controller (MKP TSC-210) and readout unit (Sehwa KRO-4001) were used to adjust and maintain the gas supply rates. Ultrahigh purity (99.99%) gases, including N₂, H₂, CO₂, and Ar, were used for all experiments. The N₂ gas was used as a carrier gas and played a role as a major discharge media. The space velocity based on the unit weight of the catalyst was 18,625 mL h⁻¹ g_{cat}⁻¹ at a total flow rate of 50 mL/min without Ar addition, whereas it was 29,800 mL h⁻¹ g_{cat}⁻¹ at 80 mL/min with Ar addition.

The moisture in the product gases was filtered through a dehydration chamber before being supplied into the gas chromatograph (YL 6100 GC, Samarth Instruments). The composition of the product gas was analyzed by gas chromatography to detect H₂, N₂, O₂, CO, CO₂, CH₄, C₂H₂, C₂H₄, C₂H₆, and C₃H₈. The definitions for conversion and selectivity are expressed in Eqs. (2)–(4); the average values of three experiments are presented, and the deviation for all values was less than $\pm 1.5\%$.

$$\text{CO}_2 \text{ conversion } (\%) = \frac{\text{Converted CO}_2}{\text{Supplied CO}_2} \times 100 \quad (2)$$

$$\text{CH}_4 \text{ selectivity } (\%) = \frac{\text{Produced CH}_4}{\text{Converted CO}_2} \times 100 \quad (3)$$

$$\text{CO selectivity } (\%) = \frac{\text{Produced CO}}{\text{Converted CO}_2} \times 100 \quad (4)$$

The OES system consists of a monochromator (Monora500i, Dongwoo Optron) and optical CCD detectors (Andor iDus DV420A-OE). The *in-situ* optical emission spectra were recorded using the Andor Solis software.

3. Results and discussion

3.1. Effect of the DBD plasma on the CO₂ conversion and CH₄ selectivity

DBD plasma-assisted CO₂ methanation was performed at atmospheric temperature and pressure. The discharge voltage and frequency were 9 kV and 3 kHz, respectively. The CO₂ conversion and CH₄ selectivity were measured when the plasma was applied in the empty reactor, when the catalyst was used without the plasma, and when both the plasma and catalyst were used simultaneously (Fig. 5 and Table 1). The CO₂ conversion and CH₄ and CO selectivity were essentially zero in the absence of the plasma. The Ru/ γ -Al₂O₃ catalyst also had no reactivity in the absence of the plasma. In contrast, a CO₂ conversion of 8.21% and CO selectivity of 43.84% were obtained using only the plasma, but the CH₄ selectivity decreased by 1.42%. However, the CO₂ conversion and CH₄ selectivity were 12.80% and 73.30%, respectively; the CO selectivity decreased when the DBD plasma was applied to the Ru/ γ -Al₂O₃ catalyst.

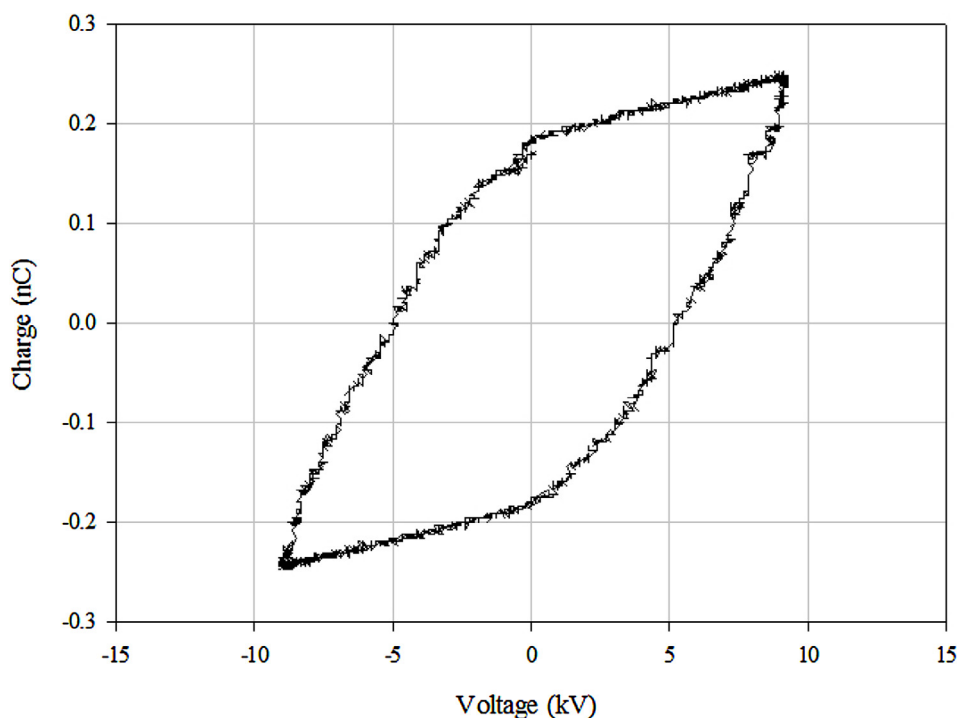


Fig. 4. Lissajous diagram of the dielectric barrier discharge (DBD) plasma discharged on Ru/γ-Al₂O₃ at 9 kV and 3 kHz.

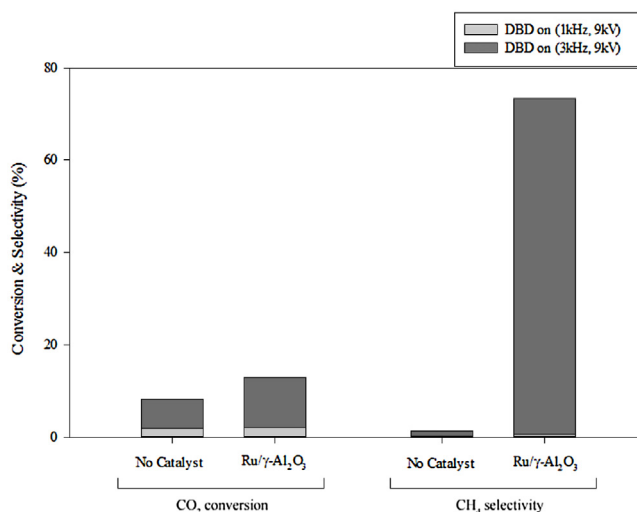


Fig. 5. Comparison of the CO₂ conversion and CH₄ selectivity at dielectric barrier discharge (DBD) plasma conditions (1 atm, 25 °C).

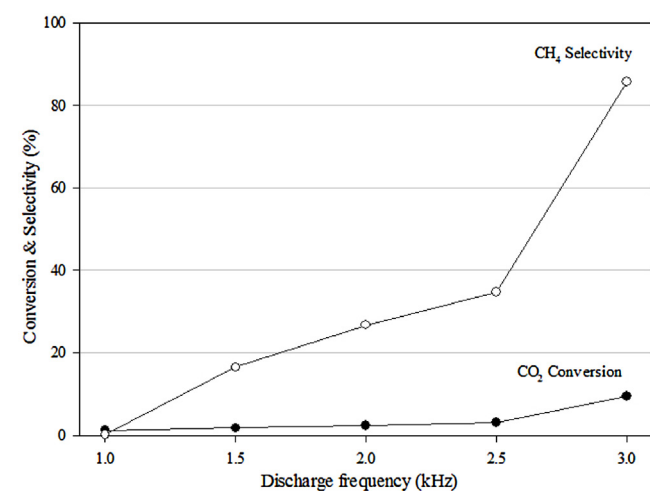


Fig. 6. Effect of the dielectric barrier discharge frequency for CO₂ conversion and CH₄ selectivity within 1.0–3.0 kHz (1 atm, 25 °C).

3.2. Effect of the discharge frequency on the activation of methanation

The effect of the discharge frequency on the CO₂ conversion and CH₄ selectivity is shown in Fig. 6. The discharge frequency increased by 0.5 kHz, while the discharge voltage was maintained at 9 kV because it was higher than the onset voltage of discharge. At 1 kHz, a small amount of CO₂ was converted to CH₄ even though the DBD plasma was generated on the Ru/γ-Al₂O₃ catalyst. However, the CO₂ conversion and CH₄ selectivity gradually increased with the increase of the discharge frequency.

The CO₂ conversion and CH₄ selectivity were directly proportional to the discharge frequency. In particular, the CH₄ selectivity suddenly increased when the discharge frequency increased from 2.5 to 3.0 kHz. The discharge frequency is a determining factor

The CO₂ conversion and CO selectivity were high but the CH₄ selectivity was low when only the plasma was applied. In contrast, the CO₂ conversion was nearly zero when only the Ru/γ-Al₂O₃ catalyst was used because the catalyst was not activated at atmospheric temperature. The CO₂ conversion and CH₄ selectivity were both high when the plasma and the catalyst were used simultaneously, but the CO selectivity significantly decreased. The results indicate that the plasma increases the deoxygenation of CO₂ and thereby enhances the activity of methanation through interactions with the Ru/γ-Al₂O₃ catalyst.

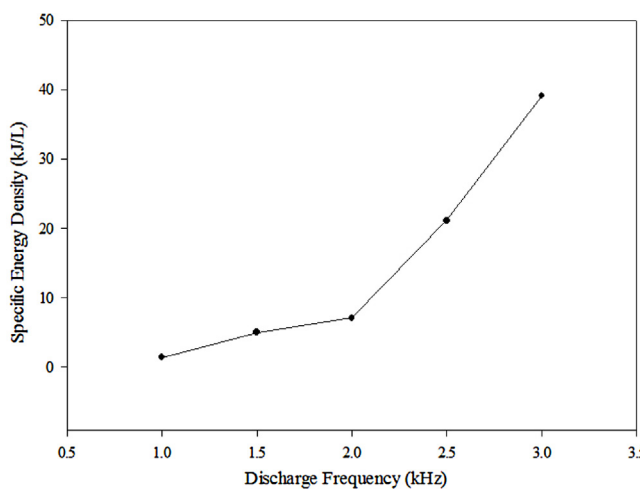


Fig. 7. Specific energy density as a function of the discharge frequency from 1.0 to 3.0 kHz.

for the energy deposition to activate methanation. The specific energy density (SED) is a function of the discharge frequency, as shown in Fig. 7. Similarly, with the tendency for CH₄ selectivity, the SED increased rapidly after a discharge frequency of 2.0 kHz was applied. CO₂ methanation was enhanced when a sufficient discharge energy was applied to the catalyst. CO₂ deoxygenation was dominant and increased the CO selectivity if either the discharge energy was lacking or the catalyst was absent.

A minimum discharge frequency is required to activate the Ru/ γ -Al₂O₃ catalyst so that it can interact with the DBD plasma. The discharge frequency is an important parameter because ionization, excitation, and radical generation can be influenced by the discharge frequency [37–39]. This discharge frequency might also be related to the aforementioned activation condition between the plasma and catalyst because a higher discharge frequency can provide more abundant ionized radicals and excited species. CO₂ deoxygenation was improved by only using the plasma, as summarized in Table 1. Thus, the plasma alone did not activate methanation. Applying the plasma to the catalyst could also satisfy the discharge condition.

3.3. Effect of the H₂/CO₂ mixture ratio

The effect of the H₂/CO₂ mixture ratio on the CO₂ conversion and CH₄ selectivity is shown in Fig. 8. N₂, which is a primary discharge media, was supplied at 30 mL/min, and the H₂/CO₂ mixture ratio was varied by adjusting the H₂ and CO₂ flow rates at a constant total flow rate (50 mL/min). The CO₂ conversion and CH₄ selectivity increased the H₂/CO₂ mixture ratio. In particular, the CO₂ conversion increased from 12.80% to 23.20% when the H₂/CO₂ mixture ratio increased from 3 to 7. At the same conditions, the CH₄ selectivity and carbon balance increased from 73.30% to 95.02%, and from 78.93% to 97.38%, respectively. However, the CO selectivity decreased as the H₂/CO₂ mixture ratio increased.

This result can be explained by the relation of deoxygenation and methanation in the H₂-rich environment provided by the high H₂/CO₂ mixture ratio. The carbon balance and CH₄ selectivity decreased but the CO selectivity increased at a low H₂/CO₂ mixture ratio. In contrast, the carbon balance and CH₄ selectivity increased at a high H₂/CO₂ mixture ratio. The carbon balance and CH₄ selectivity increased because more carbon atoms were bonded with either four hydrogen atoms or two hydrogen molecules. H₂ and CO₂ can be dissociated, ionized, or excited by electron collisions from the plasma. Therefore, at a high H₂/CO₂ mixture ratio, hydrogen can be ionized and excited by the plasma so that the ionized hydrogen

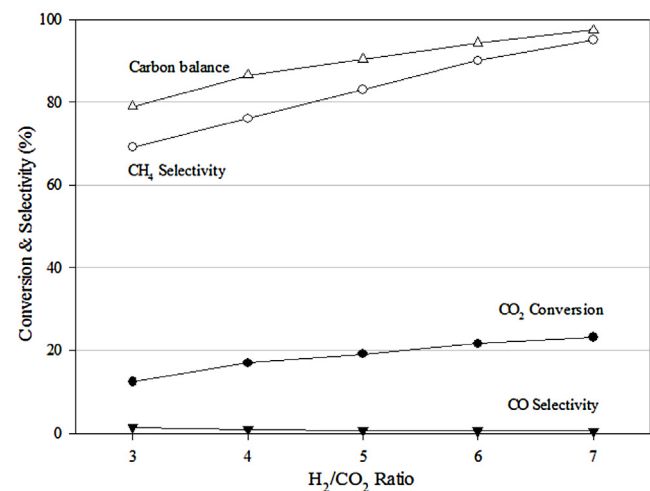


Fig. 8. Effect of the H₂/CO₂ mixture ratio on the CO₂ conversion and CH₄ selectivity for Ru/ γ -Al₂O₃ with 3 kHz and 9 kV dielectric barrier discharge (DBD) (1 atm, 25 °C).

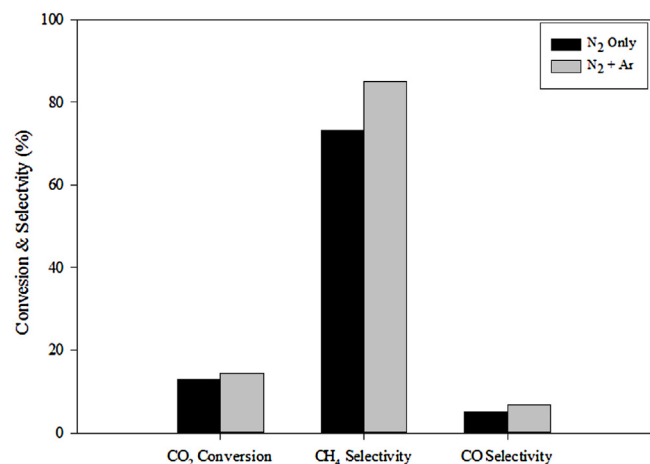


Fig. 9. Effect of N₂ and Ar added to N₂ on the dielectric barrier discharge (DBD) over Ru/ γ -Al₂O₃ with 3 kHz and 9 kV DBD (1 atm, 25 °C).

atoms and excited hydrogen molecules can actively react with CO₂ and CO, which increases the carbon balance and CH₄ selectivity. CO₂ can be dissociated to C, CO, O, and O₂ by electron collisions [40,41]. At a low H₂/CO₂ mixture ratio, C and O₂ were generated from CO₂ dissociation, but some carbon was deposited onto the catalyst surface because there was not enough chance to bond with ionized hydrogen atoms and excited hydrogen molecules. However, the plasma can generate abundantly ionized hydrogen atoms and excited hydrogen molecules, which can provide more chances for bonding with the decomposed carbons.

3.4. Effect of the addition of Ar

Ar has been widely used in various plasma applications because it is relatively easy to ionize. It has been widely used as a primary or secondary gas with N₂ because the electric discharge of the N₂/Ar mixture can increase the concentration of plasma-active species by the Penning effect [42,43]. In addition, Ar can be recycled after the methanation process because it is inert, i.e., it has not participated in the reaction, and is simply separated from product gases using either the membrane or the pressure swing adsorption process. Therefore, the N₂/Ar mixture was supplied in the reactor and the plasma discharge was performed to verify the effect of Ar addition on CO₂ methanation. Ar was added at a flow rate of 30 mL/min

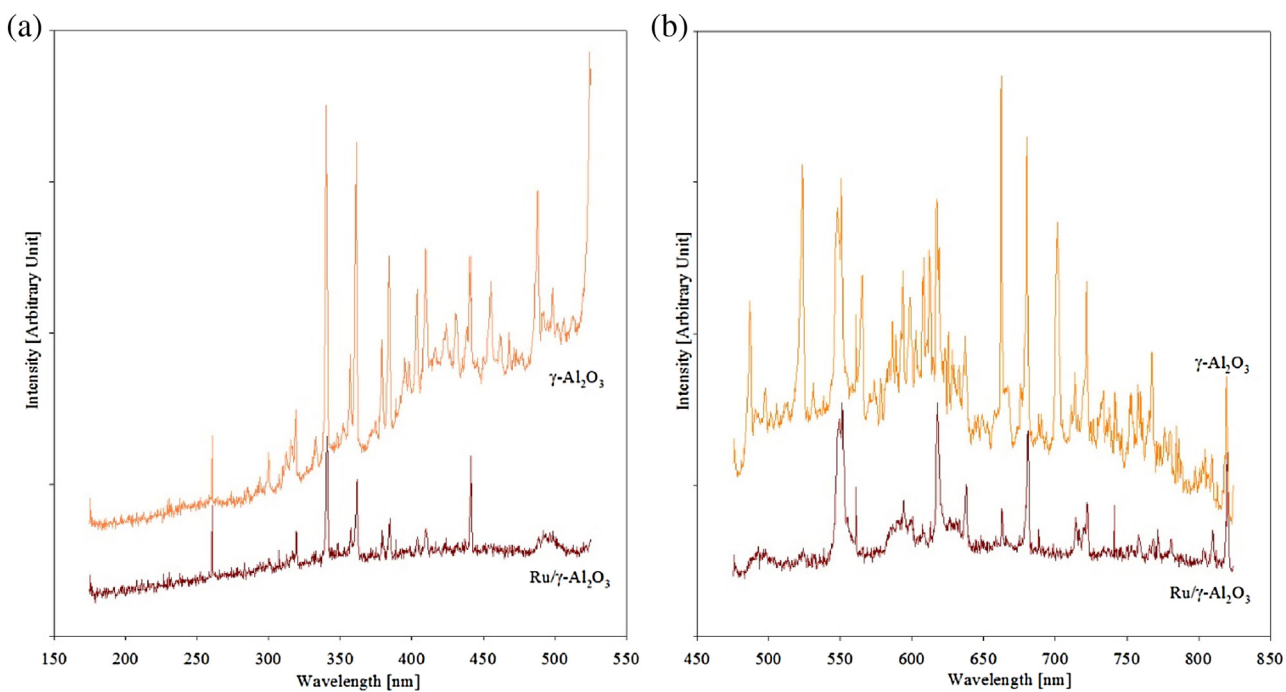


Fig. 10. Comparison of the optical emission spectra for the $\gamma\text{-Al}_2\text{O}_3$ and $\text{Ru}/\gamma\text{-Al}_2\text{O}_3$ catalysts at 3 kHz and 9 kV dielectric barrier discharge (DBD) conditions from (a) 150–550 nm and (b) 450–850 nm (1 atm, 25 °C).

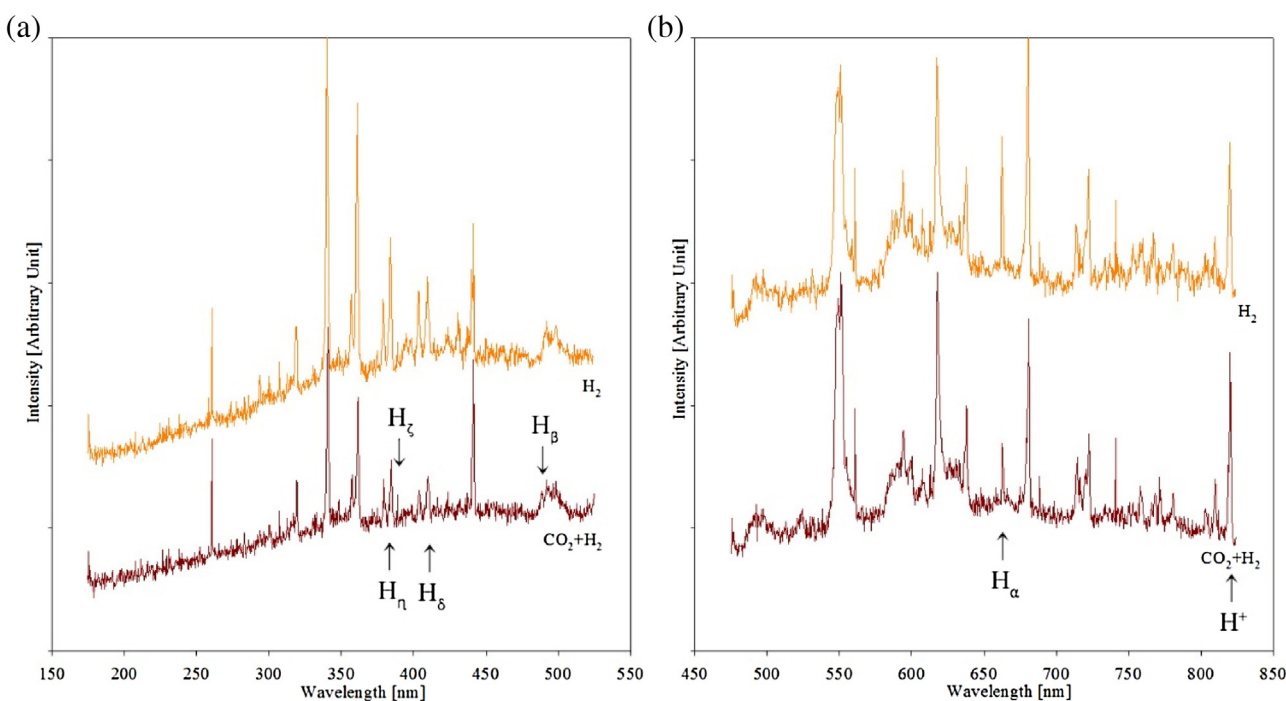


Fig. 11. Comparison of the optical emission spectra for H_2 and CO_2+H_2 mixture gas discharged over the $\text{Ru}/\gamma\text{-Al}_2\text{O}_3$ catalyst at 3 kHz and 9 kV dielectric barrier discharge (DBD) conditions from (a) 150–550 nm and (b) 450–850 nm (1 atm, 25 °C).

without changing the other flow rates (the flow rates of N_2 , H_2 , and CO_2 were fixed at 30, 15, and 5 mL/min, respectively) because N_2 is a primary discharge medium and CO_2 methanation can be affected by different gas mixture ratios. Thus, the total flow rates were different with and without Ar addition; the total flow rate was 1.6 times higher when Ar was added. The discharge conditions were identical to the other experiments (9 kV and 3 kHz).

The CO_2 conversion and CH_4 selectivity when only N_2 was used were compared with those when Ar was added to N_2 (Fig. 9). The CO_2 conversion is inversely proportional to the total flow rate. However, the CO_2 conversion with the $\text{N}_2\text{-Ar}$ discharge was higher even though the total flow rate was 60% higher than for the N_2 discharge. The CO_2 conversion increased by 1.68%, while the CH_4 selectivity increased by 11.60% in the $\text{N}_2\text{-Ar}$ discharge condition. In contrast, the CO selectivity increased by 1.72%, which means that methana-

tion and deoxygenation were simultaneously enhanced when Ar was added.

As aforementioned, the discharge can increase the concentration of the plasma active species, which leads to an increase of the electron collision frequency. As a result, this induced active CO₂ dissociation and generated more active carbons and ionized and excited hydrogens. The increased active carbon and hydrogen ions can influence both CO₂ methanation and deoxygenation because the increased electron collisions with the CO₂ species can increase deoxygenation. In addition, the increased electron collisions also induce ionization, excitation, and radical generation, which can provide more chances for carbon to bond with hydrogen.

3.5. Optical emission spectroscopy

OES is a powerful, non-contact diagnostic method to monitor excited and ionized species for plasma applications. When the excited atoms and molecules are restored to low states and the ground state, photons are released from the excited atoms and molecules; thereby, the optical emission can be detected by OES. The types of elements as well as the excitation and ionization states are determined based on the optical emission spectra of the plasma [42,44,45]. For this reasons, *in-situ* OES analysis was performed during CO₂ methanation using the Ru/γ-Al₂O₃ catalyst in the plasma.

The optical emission spectra of the γ-Al₂O₃ and Ru/γ-Al₂O₃ catalysts were measured to investigate the effect of the presence of Ru in the plasma with H₂ and CO₂ flow rates of 15 mL/min and 5 mL/min, respectively, as shown in Fig. 10. The discharge conditions were 9 kV and 3 kHz. Different emission peaks and intensities were observed in both spectra. The increased intensity of the emission bands and additional peaks were observed for γ-Al₂O₃. In contrast, several emission bands were suppressed and disappeared for the Ru/γ-Al₂O₃ catalyst. Thus, the discharge characteristics of the DBD plasma were changed by γ-Al₂O₃, thereby generating excited species with different excitation states. In addition, the presence of Ru influenced the discharge characteristics. However, the effect of the change in the discharge characteristics on the enhancement of CO₂ methanation is not clearly identified. Therefore, additional OES analyses were performed at the different gas conditions.

Optical emission spectra were recorded when the H₂/CO₂ mixture was supplied (condition for methanation) and when only H₂ was supplied (Fig. 11). The Ru/γ-Al₂O₃ catalyst was used for both cases. Similar spectra were observed in both cases, which indicate that hydrogen was mainly ionized and returned to a lower state or the ground state when the plasma was applied to the catalyst at methanation conditions. At the same time, the emission bands for the Balmer series, including H_α (656.5 nm), H_β (486.1 nm), H_δ (410.2 nm), H_ζ (388.9 nm), and H_η (383.5 nm), as well as the Paschen series of H⁺ (820 nm) were also identically detected at methanation conditions. Hydrogen radicals with different excitation states existed in the reaction because these emission series and bands are emitted from excited hydrogen atoms [46–49].

Based on the above result, we suggest that the DBD plasma provides two enhancements to CO₂ methanation: dielectric heating, and excitation and ionization by electron collisions. When the plasma was applied to the catalyst, local heating was induced by dielectric heating so that the reaction temperature could be sustained without additional heating, such as by an electric heater. Infrared thermography confirmed that the reaction temperature was maintained at 250 °C when the electric discharge was applied to the Ru/γ-Al₂O₃ catalyst at 9 kV and 3 kHz. However, dielectric heating was not a major contributor to the improvement of CO₂ methanation. In order to verify the above, CO₂ methanation was performed at the same temperature (250 °C) using the Ru/γ-Al₂O₃ catalyst without the plasma; the CO₂ conversion (3.06%)

and CH₄ selectivity (34.95%) were four times and two times lower than those with the plasma, respectively. Therefore, in addition to dielectric heating, electron collisions are a major contributor to the improvement of CO₂ methanation because the plasma provides electron collisions to generate highly reactive plasma species, such as excited and ionized hydrogen species, or dissociate oxygen from CO₂.

4. Conclusions

The DBD plasma was used to activate the Ru/γ-Al₂O₃ catalyst for CO₂ methanation at atmospheric conditions, and the effect of the interaction between the plasma and catalyst on the conversion and selectivity was investigated. The CO₂ conversion increased with the DBD plasma regardless of the presence of the catalyst at atmospheric conditions. However, when the DBD plasma was used alone, most of the CO₂ conversion was induced by CO₂ deoxygenation because CO₂ molecules were exposed to electron collisions and decomposed to CO. In contrast, the Ru/γ-Al₂O₃ catalyst was not activated without the DBD plasma. CO₂ methanation was activated when the DBD plasma was applied to the Ru/γ-Al₂O₃ catalyst. The CO₂ conversion and CH₄ selectivity increased with the increase of the discharge frequency and H₂/CO₂ ratio, and with the addition of Ar. The maximum CO₂ conversion and CH₄ selectivity were 23.20% and 97.38%, respectively, when the discharge conditions were 9 kV and 3 kHz, and the H₂/CO₂ ratio was 7.

CO₂ methanation was activated by the interaction between the DBD plasma and Ru/γ-Al₂O₃ catalyst. The OES results confirmed that the presence of the catalyst in the plasma could influence the characteristics of the plasma discharge, thereby generating highly reactive plasma species, such as the excited and ionized hydrogen species. In addition, the DBD plasma could induce dielectric heating of the catalyst and increase the catalytic activity when enough heating is provided. Therefore, the enhancement of CO₂ methanation is expected to occur by electron collisions and dielectric heating from the DBD plasma. However, the electron collisions were a major contributor because the DBD plasma could provide electron collisions to generate highly reactive plasma species, such as ionized and excited hydrogens, and dissociate carbon and oxygen from CO₂.

Acknowledgements

Funding: This research was supported by the Basic Science Research Program through the National Research Foundation of Korea (NRF) funded by the Ministry of Science, ICT and Future Planning [grant number 2014R1A2A1A11054686].

References

- [1] G. Benjaminsson, J. Benjaminsson, R. Boogh Rudberg, Powerto-gas e a Technical Review Technical Report, Svenskt Gastekniskt Center AB, Malmö, 2013.
- [2] M. Götz, J. Lefebvre, F. Mörs, A.M. Koch, F. Graf, S. Bajohr, R. Reimert, T. Kolb, Renew. Energy 85 (2016) 1371–1390.
- [3] S. Solomon, D. Qin, M. Manning, Z. Chen, M. Marquis, K.B. Averyt, M. Tignor, H.L. Miller, Contribution of Working Group I to the Fourth Assessment Report of the Intergovernmental Panel on Climate Change, Cambridge University Press, Cambridge, 2007.
- [4] P. Tans, R. Keeling, ESRL Global Monitoring Division e Global Greenhouse Gas Reference Network, 2016 [WWW Document]. URL <http://www.esrl.noaa.gov/gmd/ccgg/trends/> [Accessed 15 August 2016].
- [5] V. Jiménez, P. Sánchez, P. Panagiotopoulou, J.L. Valverde, A. Romero, Appl. Catal. A 390 (2010) 35–44.
- [6] J. Xu, X. Su, H. Duan, B. Hou, Q. Lin, X. Liu, X. Pan, G. Pei, H. Geng, Y. Huang, T. Zhang, J. Catal. 333 (2016) 227–237.
- [7] G. Garbarino, D. Bellotti, P. Riani, L. Magistri, G. Busca, Int. J. Hydrogen Energy 40 (2015) 9171–9182.
- [8] S. Danaci, L. Protasova, J. Lefevere, L. Bedel, R. Guilet, P. Marty, Catal. Today 273 (2016) 234–243.
- [9] M.S. Duyar, A. Ramachandran, C. Wang, R.J. Farrauto, J. CO₂ Util. 12 (2015) 27–33.

- [10] J. Kopyscinski, T.J. Schildhauer, S.M. Biollaz, *Fuel* 89 (2010) 1763–1783.
- [11] J.M. Panek, J. Grasser, Practical Experience Gained During the First Twenty Years of Operation of the Great Plains Gasification Plant and Implications for Future Projects, U.S. DOE, Washington, 2006.
- [12] T. Schaaf, J. Grünig, M.R. Schuster, T. Rothenfluh, A. Orth, *Energy. Sustain. Soc.* 4 (2014) 1–14.
- [13] L. Bian, L. Zhang, R. Xia, Z. Li, *J. Nat. Gas Sci. Eng.* 27 (2015) 1189–1194.
- [14] Y. Li, B.W. Jang, *Appl. Catal. A* 392 (2011) 173–179.
- [15] J. Wang, C. Liu, Y. Zhang, K. Yu, X. Zhu, F. He, *Catal. Today* 89 (2004) 183–191.
- [16] K. Li, X. Tang, H. Yi, P. Ning, Y. Xiang, J. Wang, C. Wang, X. Peng, *Appl. Surf. Sci.* 264 (2013) 557–562.
- [17] B. Roy, K. Loganathan, H.N. Pham, A.K. Datye, C.A. Leclerc, *Int. J. Hydr. Energy* 35 (2010) 11700–11708.
- [18] A. Ogata, H.H. Kim, S. Futamura, S. Kushiyama, K. Mizuno, *Appl. Catal. B* 53 (2004) 175–180.
- [19] Y.F. Guo, D.Q. Ye, K.F. Chen, J.C. He, W.L. Chen, *J. Mol. Catal. A: Chem.* 245 (2006) 93–100.
- [20] Y. Guo, D. Ye, K. Chen, J. He, *Catal. Today* 126 (2007) 328–337.
- [21] Z. Fan, K. Sun, N. Rui, B. Zhao, C. Liu, *J. Energy Chem.* 24 (2015) 655–659.
- [22] Q. Wang, B.H. Yan, Y. Jin, Y. Cheng, *Energy Fuels* 23 (2009) 4196–4201.
- [23] C.C. Chang, C.C. Hsu, C.T. Chang, Y.P. Chen, *Int. J. Hydr. Energy* 37 (2012) 11176–11184.
- [24] Y.P. Hu, G. Li, Y. Yang, X. Gao, Z. Lu, *Int. J. Hydr. Energy* 37 (2012) 1044–1047.
- [25] P.J. Lindner, R.S. Besser, *Int. J. Hydr. Energy* 37 (2012) 13338–13349.
- [26] Q. Wang, B.H. Yan, Y. Jin, Y. Cheng, *Plasma Chem. Plasma Process* 29 (2009) 217–228.
- [27] X. Tu, J.C. Whitehead, *Appl. Catal. B* 125 (2012) 439–448.
- [28] Q. Wang, H. Shi, B. Yan, Y. Jin, Y. Cheng, *Int. J. Hydr. Energy* 36 (2011) 8301–8306.
- [29] E. Jwa, S.B. Lee, H.W. Lee, Y.S. Mok, *Fuel Process. Technol.* 108 (2013) 89–93.
- [30] M. Nizio, A. Albarazi, S. Cavadias, J. Amouroux, M.E. Galvez, P. Da Costa, *Int. J. Hydr. Energy* 41 (2016) 11584–11592.
- [31] M. Nizio, R. Benrabbah, M. Krzak, R. Debek, M. Motak, S. Cavadias, E. Galvez, P. Da Costa, *Catal. Commun.* 83 (2016) 14–17.
- [32] Y. Zeng, X. Tu, *IEEE Trans. Plasma Sci.* 44 (2016) 405–411.
- [33] S. Sharma, Z. Hu, P. Zhang, E.W. McFarland, H. Metiu, *J. Catal.* 278 (2011) 297–309.
- [34] P. Panagiotopoulou, D.I. Kondarides, X.E. Verykios, *Appl. Catal. A* 344 (2008) 45–54.
- [35] I. Fechete, J.C. Vedrine, *Molecules* 20 (2015) 5638–5666.
- [36] U. Kogelschatz, *Plasma Chem. Plasma Process.* 23 (2003) 1–46.
- [37] N. Benard, E. Moreau, *Exp. Fluids* 55 (2014) 1–43.
- [38] A.A. Abdelaziz, T. Ishijima, T. Seto, N. Osawa, H. Wedaa, Y. Otani, *Plasma Sources Sci. Technol.* 25 (2016) 035012.
- [39] S.Y. Liu, D.H. Mei, Z. Shen, X. Tu, *J. Phys. Chem. C* 118 (2014) 10686–10693.
- [40] M.J. Barton, A. Von Engel, *Phys. Lett. A* 32 (1970) 173–174.
- [41] L.F. Spencer, A.D. Gallimore, *Plasma Chem. Plasma Process.* 31 (2011) 79–89.
- [42] G.L. Scheffler, D. Pozebon, *Anal. Methods* 6 (2014) 6170–6182.
- [43] N.U. Rehman, Z. Anjum, A. Masood, M. Farooq, I. Ahmad, M. Zakaullah, *Opt. Commun.* 296 (2013) 72–78.
- [44] J.W. Coburn, M. Chen, *J. Appl. Phys.* 51 (1980) 3134–3136.
- [45] S. Ghosh, V.L. Prasanna, B. Sowjanya, P. Srivani, M. Alagaraja, D. Banji, *Asian J. Pharm. Anal.* 3 (2013) 24–33.
- [46] F. Fendrych, A. Taylor, L. Peksa, I. Kratochvilova, J. Vlcek, V. Rezacova, V. Petrák, Z. Klüber, L. Fekete, M. Liehr, M. Nesladek, *J. Phys. D: Appl. Phys.* 43 (2010) 374018.
- [47] R. Bogdanowicz, *Acta Phys. Pol. A* 114 (2008) 6.
- [48] C.G. Parigger, E. Oks, *Int. Rev. Atom. Mol. Phys.* 1 (2010) 13–23.
- [49] N. Konjević, M. Ivković, N. Sakan, *Spectrochim. Acta B* 76 (2012) 16–26.